

# Excess Mutual Catalysis Is Required for Effective Evolvability

Omer Markovitch\*\*

Weizmann Institute of Science

Doron Lancet\*\*\*

Weizmann Institute of Science

**Abstract** It is widely accepted that autocatalysis constitutes a crucial facet of effective replication and evolution (e.g., in Eigen's hypercycle model). Other models for early evolution (e.g., by Dyson, Gánti, Varela, and Kauffman) invoke catalytic networks, where cross-catalysis is more apparent. A key question is how the balance between auto- (self-) and cross- (mutual) catalysis shapes the behavior of model evolving systems. This is investigated using the graded autocatalysis replication domain (GARD) model, previously shown to capture essential features of reproduction, mutation, and evolution in compositional molecular assemblies. We have performed numerical simulations of an ensemble of GARD networks, each with a different set of lognormally distributed catalytic values. We asked what is the influence of the catalytic content of such networks on beneficial evolution. Importantly, a clear trend was observed, wherein only networks with high mutual catalysis propensity ( $p_{mc}$ ) allowed for an augmented diversity of composomes, quasi-stationary compositions that exhibit high replication fidelity. We have reexamined a recent analysis that showed meager selection in a single GARD instance and for a few nonstationary target compositions. In contrast, when we focused here on composites (clusters of composomes) as targets for selection in populations of compositional assemblies, appreciable selection response was observed for a large portion of the networks simulated. Further, stronger selection response was seen for high  $p_{mc}$  values. Our simulations thus demonstrate that GARD can help analyze important facets of evolving systems, and indicate that excess mutual catalysis over self-catalysis is likely to be important for the emergence of molecular systems capable of evolutionlike behavior.

## Keywords

Evolution, networks, selection, composomes, metabolism

*A version of this paper with color figures is available online at [http://dx.doi.org/10.1162/artl\\_a\\_00064](http://dx.doi.org/10.1162/artl_a_00064). Subscription required.*

## I Introduction

The fundamental question of how primitive life emerged on the prebiotic Earth has drawn considerable scientific attention throughout the centuries [2, 5, 14, 15, 22, 42, 59, 64]. The path from organic mixtures (i.e., the primeval soup) to reproducing lifelike protocells has traditionally been dominated by two different views: the genetic, or *replicator-first*, approach, and the *metabolism-first* approach [2, 42]. Both

\* Contact author.

\*\* Department of Molecular Genetics, Weizmann Institute of Science, Rehovot 76100, Israel. E-mail: omermar@weizmann.ac.il (O.M.); doron.lancet@weizmann.ac.il (D.L.)

acknowledge the need for reliable information storage and transfer, assisted by self-replication. The replicator-first approach suggests that life began with a single self-perpetuating biopolymer (e.g., RNA) [14, 15, 18, 19, 22, 37, 42, 64], which later evolved into multimolecular networks under the replicator's control. Orgel [41] has highlighted the relationship between molecular replication and the concept of autocatalysis or self-catalysis. The metabolism-first approach suggests that the very first life precursors must have been relatively complex molecular networks arising via spontaneous accretion of simpler organic molecules [3, 9, 24, 25, 34, 48, 51, 53, 60]. In this scenario, it is further proposed that faithful reproduction directly stems from certain network attributes. Therefore, one should better understand the network properties of the implicated molecular assemblies [1, 47, 57, 66] if one can merge the two seemingly conflicting scenarios for prebiotic evolution.

One embodiment of the metabolism-first view is the lipid world scenario, which considers non-covalent assemblies of amphiphiles, such as micelles and vesicles formed by lipids [8, 39, 48, 50, 53, 69]. These are assumed to store information in the form of nonrandom molecular compositions, and pass it to progeny via homeostatic growth accompanied by fission [49]. The graded autocatalysis replication domain (GARD) kinetic model for prebiotic evolution quantitatively describes the details of such a process. It elaborates some of its evolution-related attributes [10–12, 27, 30, 44, 50, 58, 62, 67, 68], with an implied route to minimal protocells [8, 45, 49, 63, 65]. The model is based on a catalytic network, usually presented in the form of a matrix  $\beta$  with autocatalysis (self-catalysis) and cross (mutual) catalysis terms. Importantly, the system is kept away from thermodynamic equilibrium by assembly fission [49]. Key in GARD dynamics are composites—clusters of replication-prone quasi-stationary states (composomes, a term derived from the notion of compositional genomes [49]), proposed to play a crucial role in the GARD's evolutionary behavior. Introducing substantial inhibition in  $\beta$  is expected to result in net catalysis because an inhibitor of an inhibitor is an activator [20].

Catalysis, the enhancement of reaction rate by an external chemical component, was recognized as early as 1836 by Berzelius, and Ostwald applied the term *autocatalysis* in 1890 to reactions that gain speed as they proceed [26, 44]. In the genetic approach to life's origin, researchers invoke one or several autocatalytic molecules as the core of a prebiotic entity. This is exemplified by the *hypercycle*, a set of self-replicating polynucleotides, coding for and acted upon by enzymes [10, 30, 58]. In the metabolism-first domain, autopoiesis [67] and the chemoton model [12] are examples of collective autocatalysis [25].

Collectively autocatalytic systems feature a central role not only for self-catalysis, but also for mutual catalysis. In this, they arguably resemble present-day living cells, which harbor self-catalytic polynucleotides as well as a plethora of mutual catalysts that constitute metabolic pathways. Here we utilize a metabolism-first simulator to examine the relative importance of the two catalytic modes (self- and mutual catalysis). Previously [11], an abstract chemistry model has been used to demonstrate that self-maintaining organizations arise only once self-catalysis is completely inhibited [11, 62]. We attempt to extend such results in the realm of the GARD kinetic model, asking what features of the  $\beta$  network contribute to the evolution of the ensuing compositional assemblies. It is shown that excess mutual catalysis is a necessary, though not sufficient, condition for displaying several evolutionlike characteristics, including a high number of composome types, higher evolvability scores, and a significant response to selection.

Recently, it has been argued that collectively autocatalytic metabolic networks, such as the GARD, do not allow for fitter compositional genomes to be maintained by selection. Vasas et al. [68] compared the frequency ranking of random GARD compositional assemblies before and after selection, and found that the relative ranks changed only slightly. This was taken as evidence for an inherent evolutionary limitation of metabolism-first scenarios. Here it is demonstrated, based on a large number of simulations, that when quasi-stationary composomes rather than arbitrary compositions serve as selection targets, GARD networks *are* capable of a significant response to selection. Importantly, this can happen chiefly when a high proportion of mutual catalysis is present in a GARD network. The results highlight the potentially important role of mutual catalysis, as compared to self-catalysis, in the emergence of early lifelike systems.

## 2 Model and Methods

### 2.1 GARD Formalism

The regular GARD formalism describes the time-dependent dynamics of a molecular assembly, by following the fate of a compositional vector whose elements are the molecular counts  $n_i$  within the assembly:

$$v = \{n_1, n_2, \dots, n_{N_G}\} \quad (i = 1, \dots, N_G) \quad (1)$$

The vector dynamics is governed by mutually catalytic interactions among the invariable number of constituent molecule types,  $N_G$ . The assembly grows by accretion of environmental molecules, and once a limiting size  $N_{\max}$  is attained, random fission is applied, producing two progeny of the same size,  $N_{\min} = N_{\max}/2$ , one of which grows again, generating growth-fission cycles of consecutive generations. GARD dynamics is described by a set of ordinary differential equations

$$\frac{dn_i}{dt} = (\kappa_f \rho_i N - \kappa_b n_i) \left( 1 + \sum_{j=1}^{N_G} \beta_{ij} \frac{n_j}{N} \right), \quad N = \sum_{i=1}^{N_G} n_i, \quad (2)$$

where  $dn_i/dt$  is in units of the individual reaction rates at which the counts of elements are changing [49], and  $\kappa_f$  and  $\kappa_b$  are respectively the basal forward and backward rate constants (joining and leaving the assembly). Typically  $\kappa_f \gg \kappa_b$ , reflecting a high equilibrium constant  $\kappa_f/\kappa_b$  for spontaneous amphiphile accretion (Table 1). Here  $\rho_i$  is the buffered concentration of molecule type  $i$  in the environment (assumed here to be equal for all  $i$  values),  $N$  is the assembly current size, and  $\beta_{ij}$  is

**Table 1.** Simulation parameters.  $N_G$  is the number of molecular types (repertoire size);  $N_{\max}$  is the assembly pre-fission size;  $\kappa_f$  and  $\kappa_b$  are the respective basal forward and backward rate constants;  $\rho_i$  is the buffered environmental concentration of molecule type  $i$ ;  $\mu$  and  $\sigma$  are the respective mean and standard deviation of the lognormal distribution of  $\beta_{ij}$  values (Appendix A.1, Equation 12);  $GEN$  is the duration of a simulation; Lognormal random seeds is the range of random seeds used for simulations;  $L_{\text{pop}}$  is the constant size of the population in the population GARD.

$N_G$	100
$N_{\max}$	$N_G$
$\kappa_f$	$10^{-2}$
$\kappa_b$	$10^{-4}$
$\rho_i$	$1/N_G$
$\mu$	-4.0
$\sigma$	4.0
$GEN$	5,000
Lognormal random seeds	1–10,000
$L_{\text{pop}}$	1,000

the non-negative matrix element signifying the rate enhancement exerted by an assembly molecule of type  $j$  on an incoming or outgoing molecule of type  $i$

$$i_{\text{out}} + j_{\text{in}} \xrightleftharpoons[k_f \times (1 + \beta_j)]{k_b \times (1 + \beta_j)} i_{\text{in}} + j_{\text{in}} \quad (3)$$

The chemical reaction in Equation 3 embodies the notion that molecular catalysis equally affects the forward and the backward rates, obeying the constraint that a catalyst may not change the equilibrium constant of the reaction it affects. This means that even under catalytic action, the relationship  $k_f \gg k_b$  prevails.

The matrix  $\beta$  represents a network of self-catalytic (diagonal elements) and mutually catalytic (off-diagonal elements) catalytic interactions (Figure 1), with self-catalysis represented by the case  $j = i$  (Appendix A.1, Equation 13). The matrix elements are randomly drawn from a lognormal distribution (Appendix A.1 and Equation 12) [49].

## 2.2 GARD Simulations

The model is subjected to a kinetic Monte Carlo simulation based on Gillespie's algorithm [16, 17, 51] using parameter values similar to those employed in previous studies (Table 1). Simulations are run using MATLAB versions 7.6–7.10 (the GARD10 code is available upon request). A set of 10,000 GARD simulations is generated, all with the same parameters, and each with a different matrix  $\beta$  generated by the MATLAB pseudorandom number generator with seeds 1–10,000. The validity of the conclusions drawn here is ascertained by repeating the simulations with smaller data sets, with seeds 1–2,000 and 2,001–4,000, striving to verify that the entire 10,000-strong data set adequately represents the GARD simulation space. The random sampling of  $\beta$  values may be perceived as representing different possible GARD environmental chemistries.

The relative mutual catalysis power

$$p_{\text{mc}} = \frac{\sum_{i=1}^{N_G} \sum_{j=1}^{N_G} \beta_{ij}}{\sum_{q=1}^{N_G} \beta_{qq}} \cdot \frac{N_G}{N_G^2} \quad (4)$$

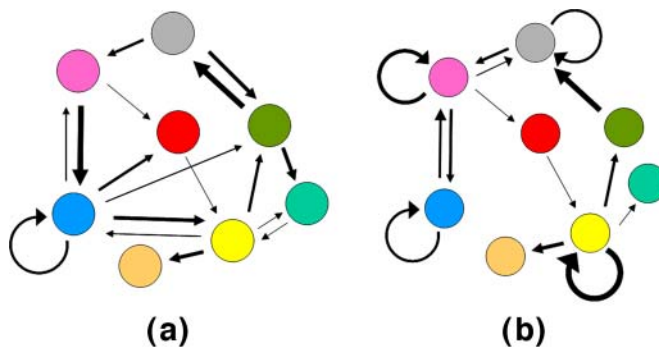


Figure 1. Network representation of GARD's  $\beta$  matrix. Two cartoon networks are shown, one with excess mutual catalysis (a) and the other with excess self-catalysis (b). In the electronic version, colored circles represent different molecular types, and arrow thickness represents catalysis strength (Equation 3). Self-catalysis is the shortest closed loop, containing one molecular type (see Appendix A.1, Equation 13).

is defined as the sum of all rate enhancements divided by the sum of self-catalysis rates (diagonal  $\beta$  elements). Because there are only  $N_G$  diagonal elements and the total number of elements is  $N_G^2$ , an appropriate correction is introduced. Thus, the excess of mutual catalysis is represented by  $p_{mc} > 1$ , while the excess of self-catalysis (or autocatalysis) is portrayed by  $p_{mc} < 1$ .

### 2.3 Compositional Similarity and Comptypes

The similarity between the compositions  $v^\chi$  and  $v^\delta$  of the respective assemblies at generations  $\chi$  and  $\delta$  is defined as the dot product  $H$  (see Equation 5) of their composition vectors [49], typically calculated at assembly size  $N_{\max}$  (end of the growth cycle).

$$H(\chi, \delta) = H(v^\chi, v^\delta) = \frac{v^\chi \cdot v^\delta}{|v^\chi| \cdot |v^\delta|} \quad (5)$$

GARD dynamics is visually portrayed by a *similarity carpet*, showing  $H$  between any pair of parent assemblies during a simulation (e.g., Figure 10 in Appendix A.4). Composomes, appearing as dense areas with high similarity near the main diagonal, are defined as any two consecutive generations where  $H(\chi, \chi + 1) \geq 0.9$  [56]. Inter-composome similarity is viewed by off-diagonal examination. The time duration of different generations (Equation 2) is different due to different growth pathways; hence a certain level of selection is already achieved by the matrix  $\beta$  causing composomes to appear more frequently than random compositions [49].

All the compositions belonging to composomes in the entire simulation undergo  $k$ -means clustering [56, 61], and the centers of mass of the resulting clusters are defined as comptypes.

### 2.4 Similarity Autocorrelation

The similarity autocorrelation function,  $c(\Delta t)$ , akin to a Fourier transform of the compositional similarity time series, is defined by

$$c(\Delta t) = \langle H(\chi, \chi) \cdot H(\chi, \delta) \rangle = \langle H(\chi, \delta) \rangle \quad (6)$$

where  $\langle \dots \rangle$  denotes averaging over all generation pairs fulfilling  $\delta - \chi = \Delta t$ . This function is history independent, that is, no conditions are imposed on the events occurring between generations  $\chi$  and  $\delta$ .

$c(\Delta t)$  is fitted with a single exponential with parameters  $\tau$  and  $H_0$  using a least squares fit (see Appendix A.2, and Figure 12 in Appendix A.4):

$$c(\Delta t) = (1 - H_0) \exp\left(-\frac{\Delta t}{\tau}\right) + H_0 \quad (7)$$

The parameters  $\tau$  and  $H_0$  are used to define a measure of evolvability (Section 3).

### 2.5 Selection in GARD

For each simulation, the most frequent comptype is chosen as a target,  $T$ . A selection-GARD simulation is then run, whereby the growth of an assembly at generation  $\chi$  is biased toward  $T$  via a growth bonus parameter

$$G_b = s \cdot H(v^\chi, T) \quad (8)$$

manifested as a temporary enhancement of the corresponding  $\beta_{ij}$  values, as suggested [68], where  $s > 1$  is a fitness gain, embodying a selective advantage, and for consistency with previous work [68]  $H(v^\chi, T)$  is calculated at assembly size  $N_{\min}$ , that is, the beginning of the growth cycle.

The modified matrix element  $\beta'_{ij}$  is obtained at each generation according to

$$\beta'_{ij}(\chi) = \begin{cases} \beta_{ij}, & i \text{ or } j \notin \nu^\chi \\ G_b \cdot \beta_{ij}, & i \text{ and } j \in \nu^\chi \end{cases} \quad (9)$$

where  $i$  and  $j$  are molecular type indices, and  $\beta_{ij}$  modification is effected for all  $i,j$  (and  $j,i$ ) pairs contained within the current assembly. Thus, the network will be perturbed only at edges present within the current assembly according to how similar the current assembly is to the target. In the selection-GARD simulation, a comptype  $T'$  is identified as having the highest  $H$  value with respect to  $T$ . An unambiguous identification of  $T'$  is afforded by the fact that the mean similarity between  $T$  and  $T'$  in the entire data set is  $H = 0.9933 \pm 0.0217$ . The selection excess is subsequently defined as

$$SE = \frac{f_{T'}}{f_T} \quad (10)$$

where  $f_{T'}$  and  $f_T$  are the fractions of generations belonging the respective comptype (before and after selection). Selection excesses  $\geq 1.05$  and  $\leq 0.95$  are respectively taken to represent positive and negative target selection; the rest are taken to signify no selection.

## 2.6 Selection Dynamics in a Population of Compositional Assemblies

An initially random population of a fixed number of assemblies,  $L_{\text{pop}}$ , is allowed to simultaneously grow according to Equations 1 and 2 and its idiosyncratic composition. When one of the assemblies reaches the limiting size  $N_{\text{max}}$ , it divides by random fission, and a randomly chosen assembly from among the other  $L_{\text{pop}} - 1$  assemblies is removed, thus keeping the population size constant. This is repeated for GEN splits (Table 1). This protocol is based on the classical Moran process [36, 68, 70], and to some degree reflects an earlier attempt to simulate GARD populations [38].

The frequency of the target in each population is defined as the number of assemblies that are highly similar ( $H \geq 0.9$ ) to the target comptype taken from regular GARD for the same  $\beta$  network (Figure 13 in Appendix A.4). Selection is exerted by performing a simulation with the same parameters, biasing the growth of assemblies toward a target comptype as for regular GARD (Equations 8 and 9). The selection excess is defined as in Equation 10, where  $f_{T'}$  and  $f_T$  are respectively the fractions of assemblies within the population belonging to the target comptype before and after selection.

## 3 Results

### 3.1 Selection in GARD

We used GARD simulations to ask what is the selection response of compositional assemblies. A value for the selection excess was obtained for each of 10,000 simulations, using a modest value of the fitness gain,  $s = 1.1$ , in line with previous work [68]. Figure 2a shows the correlation between the frequencies of the target comptype with and without selection (examples of regular GARD carpets before and after selection are given in Figure 14 in Appendix A.4). An overall skew is seen here toward positive selection. The figure also demonstrates that significant positive selection, as well as negative, occurs over most of the range of  $f_T$ :

Figure 2b shows the distribution of selection excess values for the entire data set (Equation 10). Importantly, a considerable percentage of the simulations (33%) show positive selection, with a mean selection excess of 1.38 for selection excess  $> 1.05$ , and as much as 10% shows selection excess  $> 1.5$ . Interestingly, 31% of the cases showed negative selection, with a mean selection excess of 0.775 for selection excess  $< 0.95$ , and about 36% were neutral to the selection pressure. Similar to the skewness in Figure 2a, there is a slight bias in favor of positive selection, as indicated by an overall mean selection

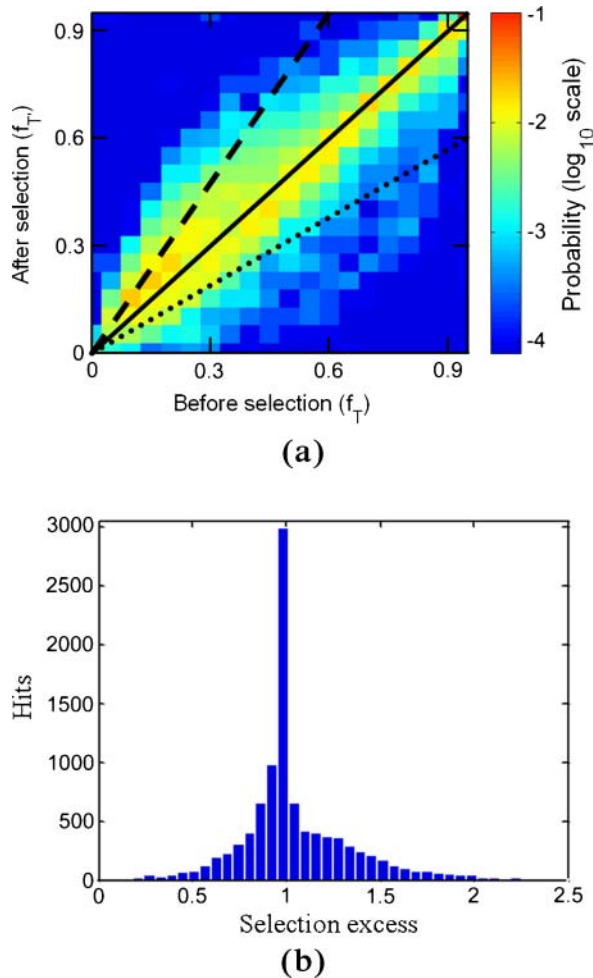


Figure 2. Selection in GARD. (a) The correlation between the frequencies of the target comptotype in the basal simulation ( $f_T$ ) and its frequency after applying selection ( $f_T'$ ). In the electronic version, color represents probability out of the entire data set of 10,000 simulations, and positive and negative selection are respectively seen above and below the diagonal (selection excess = 1.0, solid black line). The dashed and dotted lines respectively mark selection excesses of  $\frac{3}{2}$  and  $\frac{1}{2}$ . (b) Selection excess histogram for the entire data set. Simulation parameters are given in Table 1.

excess equal to 1.05. Notably, higher mean selection values positively correlate with the number of other comptotypes coexisting with the target comptotype in a given system (Figure 15 in Appendix A.5).

GARD simulations are used to see how attributes of the catalytic network embodied in the matrix  $\beta$  govern the evolution-related dynamics of compositional assemblies. It is asked how the mutually catalytic power  $p_{mc}$  (Equation 4) influences the selection response. A clear trend appears here, whereby strong positive or negative selection is found almost entirely for  $p_{mc}$  higher than 1 (Figure 3b).

The main trends appear also at lower simulation counts, barring small-number fluctuations at high  $p_{mc}$  (Figure 3a). For example, for the range of  $p_{mc} > 100$ , a meaningful  $p$ -value with 5% significance level is achieved only after performing more than 2,500 simulations (Table 3 in Appendix A.6). The other two evolution-related parameters withstand similar scrutiny (below).

### 3.2 Populations of GARD Assemblies

The foregoing simulations of the regular GARD model addressed the case in which at each time point only one GARD assembly is considered. To enhance the capacity to draw conclusions about

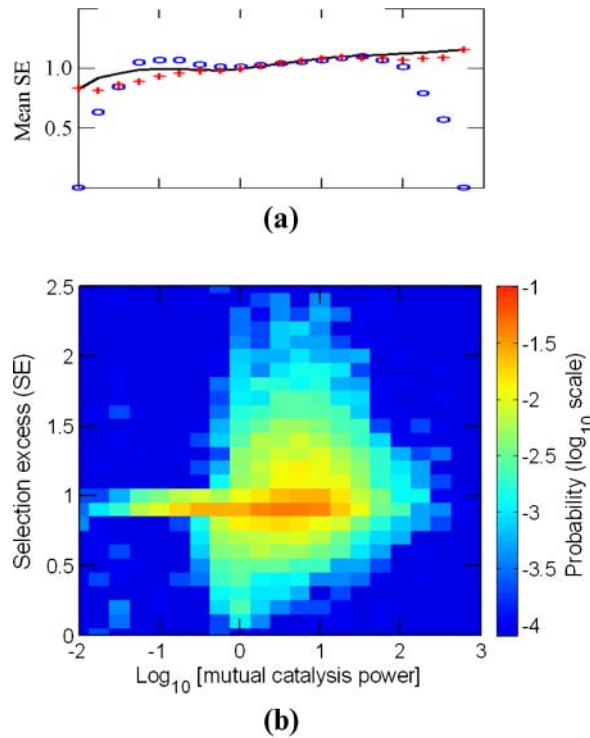


Figure 3. The dependence of selection excess (SE) on mutual catalysis power ( $p_{mc}$ ). (a) Mean SE versus  $\log_{10} p_{mc}$ , collected from 10,000 GARD instances (solid black line, smoothed) or from two subsets of 2,000 instances, random seeds 1–2,000 (ovals) and 2,001–4,000 (crosses). (b) Density plot of SE versus  $\log_{10} p_{mc}$ . In the electronic version, color represents probability of finding instances with specific (SE,  $p_{mc}$ ) values in all 10,000 GARD instances. Data is the same as in Figure 2.

selection in GARD, 1,000 simulations were performed, each for a population of 1,000 assemblies, under the constant population conditions. Figure 4 shows an example of the dynamics for one of the networks. Starting from a population of random assemblies, the population frequency of the target compotype gradually grows over the first 10,000 split events, reaching a plateau with fluctuations, signifying the compositional preference imposed by the matrix  $\beta$  towards this compotype. When selection toward this compotype is applied (Equation 9), this general behavior is retained, with a faster

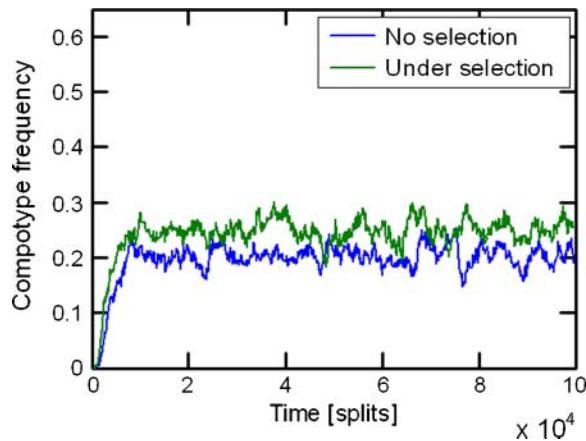


Figure 4. An example of the development of a compotype in population dynamics, without and with selection. This figure shows the fraction of assemblies in the population that are highly similar to a given compotype (see Section 2 and Figure 13 in Appendix A.4) over a large number of splits. Simulation parameters are lognormal seed = 3, GEN = 100,000, and the rest are given in Table I.

growth and a higher plateau, that is, showing positive response to selection. Similar to Figure 3b, strong positive or negative selection is much more prevalent for  $p_{mc}$  values higher than 1 (Figure 5b).

The effect of selection pressure on the frequency of the target compotype for all 1,000 networks is presented in Figure 5a. Similarly to Figure 2a, an overall skew toward positive selection is seen (about 50% of cases), with some cases of negative (about 15% of cases) or no response to selection, and with a mean selection excess of  $1.254 \pm 0.804$ . Significantly, the ratio of the number of simulations showing positive selection to that showing negative selection increased more than threefold, from 1.06 in the regular GARD to 3.33 in the population-GARD. In line with previous work [68], the growth bonus was calculated when the assembly size was  $N_{min}$  (Equation 8). When the bonus was calculated for all time points between  $N_{min}$  and  $N_{max}$  (for a smaller set of 100 population-GARD simulations), the overall selection response seems to become even more positive (70% of cases), with a higher selection excess value of  $1.399 \pm 0.997$ .

### 3.3 Compotype Diversity

The influence of  $p_{mc}$  on one of the attributes of GARD diversity, the mean number of different comptypes appearing in a simulation, is now analyzed. It is found that as  $p_{mc}$  increases, so does the mean

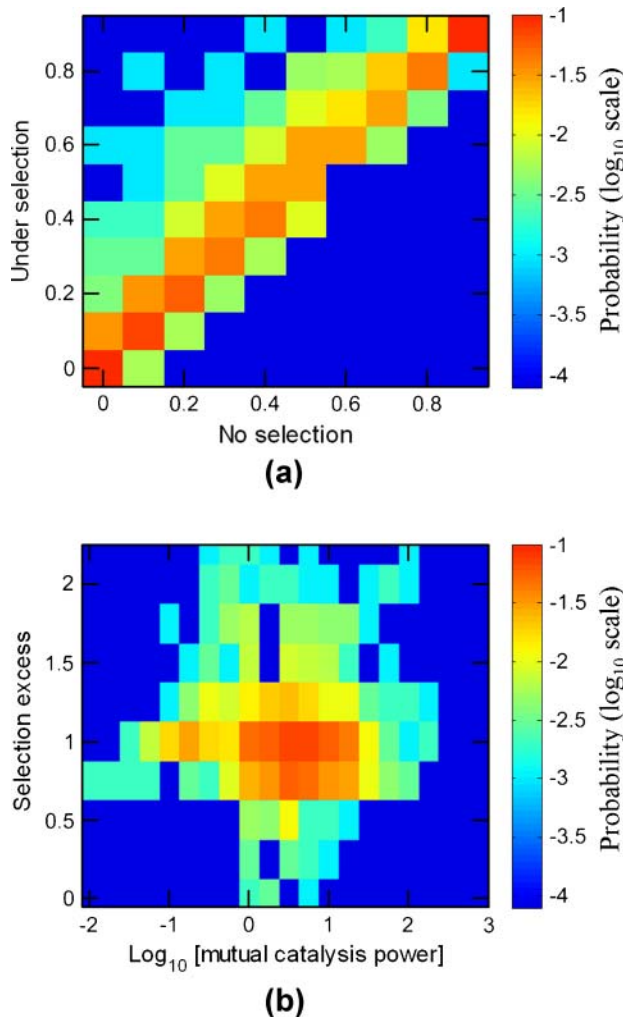


Figure 5. Selection in population-GARD. Figure details for (a) and (b) are as in Figures 2a and 3b, respectively. Data set is 1,000 population-GARD simulations, whose parameters are collected in Table 1.

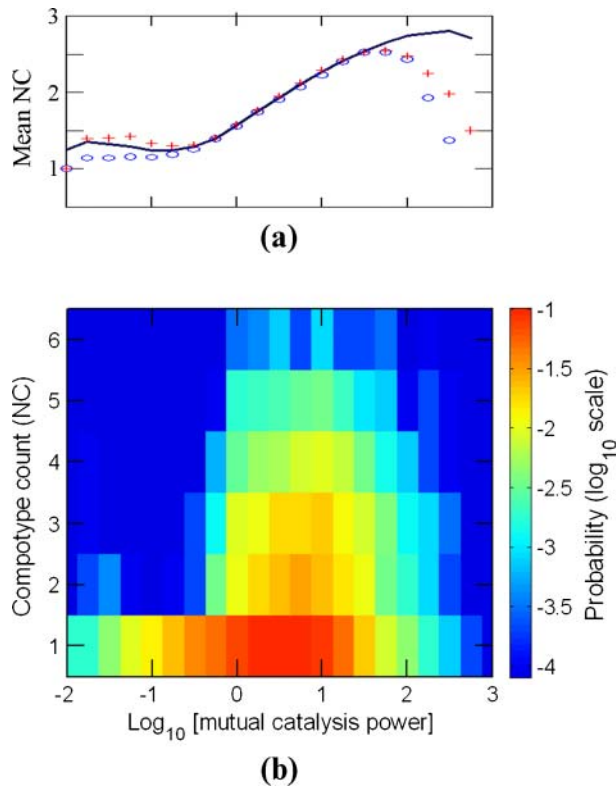


Figure 6. The dependence of compotype count (NC) on  $p_{mc}$ . Details are as in Figure 3.

number of compotypes, reaching a maximal value of nearly 3 at  $p_{mc} = 100$  (Figure 6a). Furthermore, in the realm of excess self-catalysis ( $p_{mc} < 0.5$ ), one compotype appears in an overwhelming majority of the cases (91%) (Figure 6b). In contrast, compotype counts between 2 and 6 are almost entirely confined to the domain of excess mutual catalysis ( $p_{mc} > 2$ ). Curiously, even among the  $\sim 5,000$  simulations that show only one compotype, a large majority have  $p_{mc} > 2$ , suggesting that high mutual catalysis is a necessary but not sufficient condition for a high number of compotypes.

### 3.4 GARD Evolvability

The similarity autocorrelation function (Equation 6) and its derived parameters (Equation 7) are employed to obtain information on the evolutionlike dynamics of GARD assemblies. One possible interpretation of the value of  $\tau$  is a depiction of the whole-simulation average of the assembly compositional lifetime. Longer  $\tau$  may be taken to represent better average maintenance of compositional similarity between consecutive GARD generations, symbolizing better reproduction fidelity. Likewise,  $1/\tau$  may be thought of as related to the compositional mutation rate. Indeed, effective compositional preservation is implicated by the most frequent number of generations,  $\tau \approx 3$ , with a non-negligible probability for  $\tau \geq 10$  (Figure 7a). Note that  $\tau$  does not represent the compositional lifetime. In fact, the most probable target compotype lifetime (taking for simplicity the maximal time from each simulation) is 30, and the average is 434 generations (Figure 7c). The other similarity autocorrelation parameter,  $H_0$ , is interpreted here as showing the residual compositional similarity among assemblies along many generations in the entire simulation. Thus,  $1 - H_0$  is taken as proportional to the overall compositional diversity of assemblies across the entire simulation. Note that  $H_0$  is not strongly correlated with the compotype count (Figure 16 in Appendix A.5, correlation coefficient  $-0.049$ ,  $r^2 = 0.89$ ) and therefore constitutes a rather independent diversity assessment attribute. The most probable  $H_0$  value is  $\sim 0.5$ , with a smaller probability peak at  $H_0 \approx 1$ . The latter stems from simulations in which a single compotype tends to dominate.

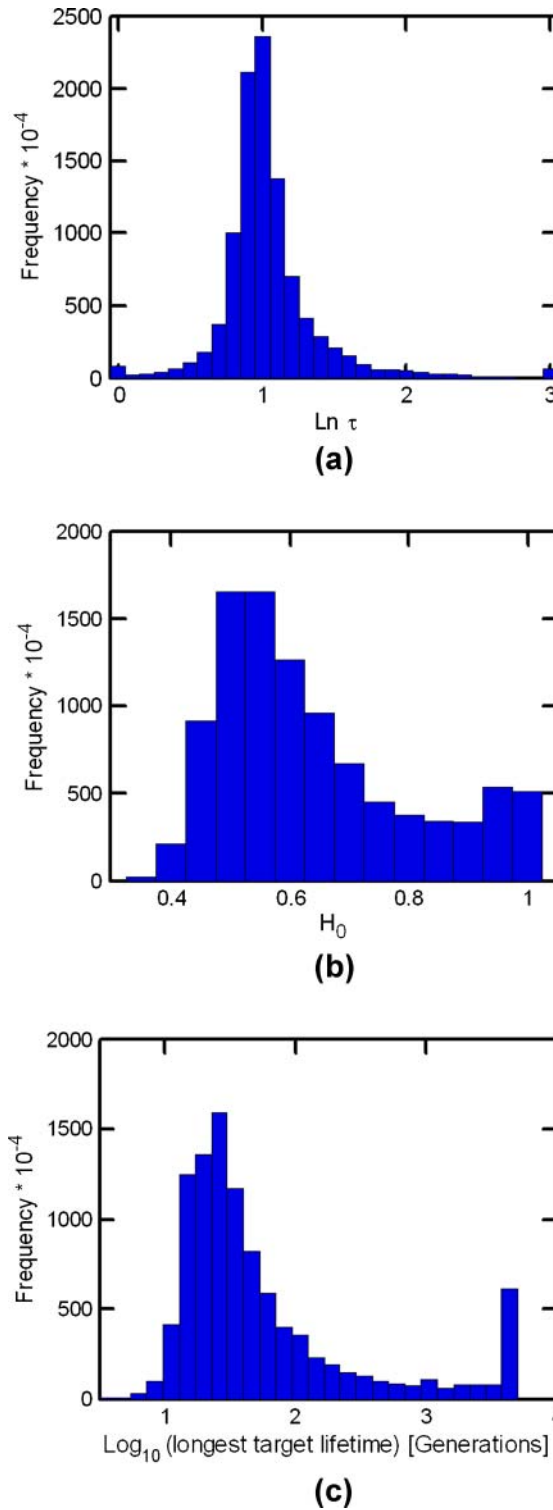


Figure 7. Distributions of  $\tau$ ,  $H_0$ , and composome duration. (a) A histogram of  $\tau$ : unit is number of generations, and the rightmost bin represents all data with  $\ln \tau > 3$ . (b) A histogram of  $H_0$ , unitless. (c) Distribution of the longest appearance of target compotypes. Data in panels is the same as in Figure 2.

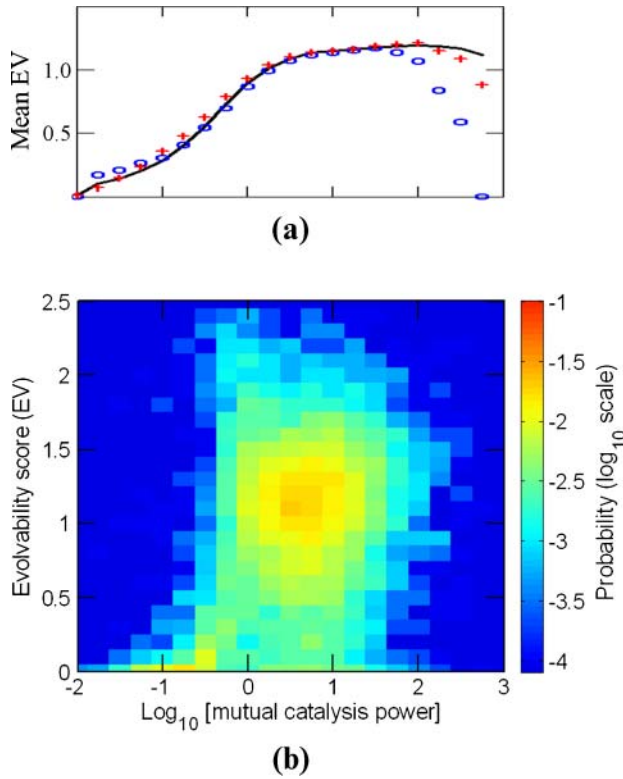


Figure 8. The dependence of the evolvability score (EV) on  $p_{mc}$ . Details are as in Figure 3.

A score is defined, which could arguably assess a GARD system’s evolvability:

$$EV = \tau(1 - H_0) \tag{11}$$

A larger evolvability score will typically arise when the system concomitantly displays appreciable trans-generation compositional preservation and higher overall compositional diversity. This compound

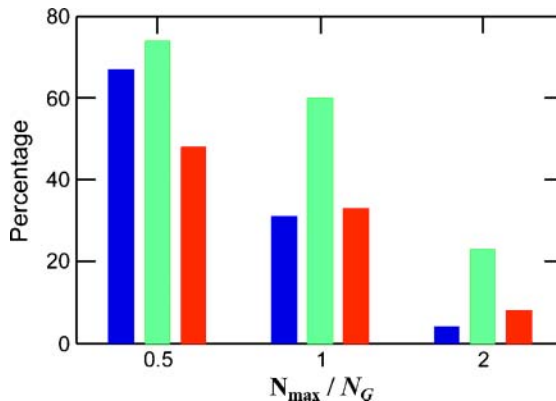


Figure 9. The percentage of regular-GARD instances exhibiting extreme evolution-related parameters as a function of maximal assembly size ( $N_{max}$ ). In the electronic version, the values taken are: comotype count >2 (blue), evolvability score >1 (green), and selection excess >1 (red). All parameters, except  $N_{max}$ , are as in Figure 3b. Full histograms and their related data are given in Appendix A.6 (Figure 17 and Table 3).

measure reflects similar definitions of evolvability [7, 43]. Similar to the selection excess and number of compotypes, a clear trend appears, whereby high evolvability scores are much more prevalent for  $\beta_{mc}$  values higher than 1 (Figure 8).

### 3.5 The Effect of Assembly Size

The effect of the assembly pre-fission size  $N_{max}$  on GARD's evolutionlike behavior was studied by performing two additional sets of 10,000 simulations, each with the same parameters as in Table 1 except for  $N_{max} = N_G/2$  and  $2N_G$  (Figure 9; Figure 17 and Table 3 in Appendix A.6). While for the smaller  $N_{max}$  value, the percentage of beneficial outcomes seems to be even higher than for the nominal  $N_{max} = N_G$ , a larger  $N_{max}$  value appears to have a disruptive effect because the system is nearing the equilibrium steady state [23]. This is especially seen for the compotype count and the evolvability score.

## 4 Discussion

### 4.1 The Significance of Mutual Catalysis

One of the dominant concepts in prebiotic evolution research is the replicator-first scenario [10, 32, 40]. Based on the concept that molecular replication is related to self-catalysis [41], such views may be perceived as related to the RNA-first scenario, positing that life began with a unique self-replicating polyribonucleotide. In this realm, it is argued that more complex interaction networks have arisen only at later stages, as when precursors for the autocatalytic molecule have been exhausted [31]. Our simulation results demonstrate an advantage for a network-first scenario, in which a large number of molecular components mutually interact. While arising from a metabolism-related framework, such results may be taken as relevant to the question of whether life's early precursors were a set of replicators or a metabolic network. Note that the present work makes a direct comparison between a metabolic network with frequent self-catalytic interactions and a metabolic network with frequent mutually catalytic interactions, and therefore has only indirect relevance to the question of the validity of replicator models. It is conceivable that future work incorporating templating biopolymers together with mutually catalytic networks will better resolve this issue.

A widespread argument against metabolism-like entities being the first seed of life is the assertion that metabolic networks cannot store and propagate information. The GARD model may be viewed as a counterexample, as it is endowed with a (limited) capacity to store and propagate compositional information. This has implications for a set of previously proposed models involving networks of molecular interactions. Two of the earliest relevant concepts are Gánti's chemoton [12, 13, 63] and Maturana and Varela's autopoietic systems [35, 67]. Autopoiesis characterizes a spatially confined network of molecular components, whose mutual interactions continuously regenerate the network itself. The chemoton is described as a system of three subnetworks: metabolite generation, template copying, and membrane synthesis. We prudently suggest that GARD may be viewed as a special case of autopoietic-chemoton-like models, where template copying and compartmentation are embodied in one entity, and a continuous supply of metabolites is afforded by the spontaneous accretion of lipids from the buffered environment.

### 4.2 The Effect of Mutual Catalysis on GARD Diversity and Evolvability

An important result of this work is that networks within a certain range of kinetic parameters, namely those that exhibit excess mutual catalysis, lead to enhanced diversity and evolvability of GARD compotypes. The compotype count is a direct indication of the degree of compositional diversity. This result is related to an important aspect of early evolution: Self-catalysts tend to propagate their own identity and suppress processes essential for the increasing complexity necessary for transitions from early seeds of life toward systems resembling present-day life. The presently demonstrated importance of mutual catalysis echoes the notion of systems prebiology [21, 57], whereby it is suggested that life began its trajectory from complex chemical mixtures obeying network behavior similar to that of metabolism in present-day cells.

### 4.3 Compotypes as Selection Targets

One of the unique corollaries of the GARD model is the emergence of composomes, dynamic states of compositional assemblies that embody both metabolism-like characteristics and a rudimentary capacity to store and propagate molecular information [49]. Composomes may be considered as forming bridges between seemingly disparate views of the early seeds of life: metabolism first and replicators first. Compotypes are further defined as centers of mass of composome clusters, which may be regarded as analogous to species or quasi species [6]. This is due to the fact that a compotype is a distinct entity, with distinct physical properties and hence fitness encoded in its compositional information, different from those of other compotypes but still harboring considerable internal variability of constituents. Therefore, compotypes are considered as natural targets of selection, as compared to randomly chosen compositions, as previously pursued [68]. Note that here we have a measure of selection inherently present in the GARD model even in the absence of external selective pressure, due to the fact that different composomes have different average growth rates. This is seen in the present population GARD simulations, which are seeded with a random population, but show a gradual increase of the population frequency of a specific compotype even in the absence of externally imposed selection. This increase comes at the expense of other compositions because of the constant population condition.

### 4.4 Selection in a GARD

The present results show that GARD assemblies can exhibit positive or negative selection toward a compotype target, as well as no selection at all. While in regular GARD the overall average selection excess is merely 1.05, it is noteworthy that as many as 10% of the simulations show high selection excess,  $>1.5$ . Importantly, these general results are borne out both in simulations of the regular model and in simulations involving populations of assemblies. Previously, GARD population dynamics has been studied by addressing various emergent properties, including a comparison of finite and infinite chemical environments [38]. Another study [70] showed that compositional inheritance also emerges in the GARD model variants involving assembly populations and spatial proximity interaction effects, and that it emerges in both a thermodynamic and a kinetic interaction regimen.

Analyzing GARD, both positive and negative selections can be observed in practice only when the underlying network exhibits mutual catalysis excess. This conclusion is strengthened by its demonstration in two different simulation modes: in the regular model and in populations. Notably, positive selection is observed appreciably more often in population GARD simulations, perhaps reflecting the advantage of addressing populations of competing entities with different reproductive rates. Furthermore, this selection response tends to be augmented as the number of coexisting compotypes increases in a given simulation, which may indicate a capacity of selective forces to provide an edge to the target compotype in inter-compotype competition. Further in-depth analyses (currently underway) of the ultrastructure of the  $\beta$  network, as well as subnetworks (quasi compartments [68]), could lead to a better understanding of the influence of  $p_{mc}$  and the compotype count on selection.

The present method for biasing the growth rate of a GARD target composition is in principle similar to that used previously [68]. In both cases, modifications are in effect introduced to  $\beta$  matrix elements. However, the previous analysis utilizes an interim formalism, the Eigen equation, for replication-mutation dynamics [10], and the selection-related modification is exerted by multiplying the growth rate by  $fH$ , defined in the same way as in Equation 8. The method utilized here involves direct modification (Equation 9), a possible explanation for the discrepant results obtained by the two reports. There are, however, additional significant differences between the two studies: (a) a pre-fission value  $N_{max} = 100$  used here, as compared to  $N_{max} = 6$  used previously, an obligatory small value required for the realistic application of Eigen's formalism with the available computing power; (b) a large difference in repertoire size ( $N_G = 100$  here versus  $N_G = 10$  in the earlier study); (c) the performance here of 10,000 random simulations, considered essential for proper statistical rigor, as compared to only a single simulation done previously. Both points (b) and (c) provide a significant edge to the present simulations in sampling the  $\beta$  interaction space, which allows drawing conclusions

with higher certainty. In the future it will be interesting to consider additional methodologies to exert external selection. One could be a variant of the presently used method, whereby the  $\beta$  network will be biased by a constant factor and not employing target similarity-oriented bias. Another could be biasing the environmental concentration  $\rho_i$  (Equation 2) by a constant factor based on the molecules that are contained in the target compotype.

## 5 Conclusion

The GARD model embodies the inheritance of compositional information in the realm of a lipid world scenario for early evolution [20, 21, 23, 27, 48, 49, 51, 55–57]. The GARD has recently been pursued in several additional publications [20, 39, 68, 70] and has been chosen as an archetypal metabolism-first realization [68]. This suggests that despite being a simulated toy model, the GARD has sufficient complexity to shed light on some important questions in the field of prebiotic origins. In the present work an attempt is made to shed further light on some of the GARD's evolutionary features. It is expected that the present insights will become instrumental in further efforts to extend the GARD beyond the monomer world [54], as has been preliminarily explored [55]. This might be necessary to reveal the capacity of the GARD model to capture the much-needed open-ended attributes of natural selection and evolution.

## Acknowledgments

We thank Raphael Zidovetzki and Tsviya Olender for enlightening comments, Aron Inger for assistance in coding, and Ágnes Tóth Petróczy, Azhar Ali Shah, Hugues Bersini, Leong Ting Lui, and Natalio Krasnogor for discussions. This work is partly supported by EU-FP7 project MATCHIT and by the Crown Human Genetics Center at the Weizmann Institute of Science.

## References

1. Alon, U. (2007). Network motifs: Theory and experimental approaches. *Nature Reviews Genetics*, 8(6), 450–461.
2. Anet, F. A. (2004). The place of metabolism in the origin of life. *Current Opinion in Chemical Biology*, 8(6), 654–659.
3. Bachmann, P. A., Luisi, P. L., & Lang, J. (1992). Autocatalytic self-replicating micelles as models for prebiotic structures. *Nature*, 357, 57–59.
4. Barabas, B., Tóth, J., & Palyi, G. (2010). Stochastic aspects of asymmetric autocatalysis and absolute asymmetric synthesis. *Journal of Mathematical Chemistry*, 48(2), 457–489.
5. Bedau, M. A. (2010). An Aristotelian account of minimal chemical life. *Astrobiology*, 10(10), 1011–1020.
6. Biebricher, C. K., & Eigen, M. (2006). What is a quasispecies? *Current Topics in Microbiology and Immunology*, 299, 1–31.
7. Brookfield, J. F. Y. (2009). Evolution and evolvability: Celebrating Darwin 200. *Biology Letters*, 5(1), 44–46.
8. Chen, I. A., & Walde, P. (2010). From self-assembled vesicles to protocells. *Cold Spring Harbor Perspectives in Biology*, 2/7/a002170.
9. Dyson, F. J. (1982). A model for the origin of life. *Journal of Molecular Evolution*, 18(5), 344–350.
10. Eigen, M., & Schuster, P. (1977). Hypercycle—Principle of natural self-organization. A. Emergence of hypercycle. *Naturwissenschaften*, 64(11), 541–565.
11. Fontana, W., & Buss, L. W. (1994). What would be conserved if “the tape were played twice”? *Proceedings of the National Academy of Sciences of the U.S.A.*, 91(2), 757–761.
12. Gánti, T. (1975). Organization of chemical reactions into dividing and metabolizing units—Chemotons. *Biosystems*, 7, 15–21.
13. Gánti, T. (1997). Biogenesis itself. *Journal of Theoretical Biology*, 187(4), 583–593.
14. Gesteland, F. R., Cech, R. T., & Atkins, F. J. (1999). *The RNA world* (p. 709). Cold Spring Harbor, MA: Cold Spring Harbor Laboratory.
15. Gilbert, W. (1986). Origin of life—The RNA world. *Nature*, 319, 618–618.

16. Gillespie, D. T. (1976). General method for numerically simulating stochastic time evolution of coupled chemical reactions. *Journal of Computational Physics*, 22(4), 403–434.
17. Gillespie, D. T. (1977). Master equations for random walks with arbitrary pausing time distributions. *Physics Letters A*, 64(1), 22–24.
18. Hayden, E. J., von Kiedrowski, G., & Lehman, N. (2008). Systems chemistry on ribozyme self-construction: Evidence for anabolic autocatalysis in a recombination network. *Angewandte Chemie—International Edition*, 47(44), 8424–8428.
19. Hughes, R. A., Robertson, M. P., Ellington, A. D., & Levy, M. (2004). The importance of prebiotic chemistry in the RNA world. *Current Opinion in Chemical Biology*, 8(6), 629–633.
20. Hunding, A., Kepes, F., Lancet, D., Minsky, A., Norris, V., Raine, D., Sriram, K., & Root-Bernstein, R. (2006). Compositional complementarity and prebiotic ecology in the origin of life. *Bioessays*, 28, 399–412.
21. Inger, A., Solomon, A., Shenhav, B., Olender, T., & Lancet, D. (2009). Mutations and lethality in simulated prebiotic networks. *Journal of Molecular Evolution*, 69(5), 568–578.
22. Joyce, G. F. (2002). The antiquity of RNA-based evolution. *Nature*, 418, 214–221.
23. Kafri, R., Markovitch, O., & Lancet, D. (2010). Spontaneous chiral symmetry breaking in early molecular networks. *Biology Direct*, 5(38). doi: 10.1186/1745-6150-5-38
24. Kaneko, K. (2002). Kinetic origin of heredity in a replicating system with a catalytic network. *Journal of Biological Physics*, 28(4), 781–792.
25. Kauffman, S. A. (1993). *The origins of order: Self organization and selection in evolution*. Oxford, UK: Oxford University Press.
26. Laidler, K. J. (1986). The development of theories of catalysis. *Archive for History of Exact Sciences*, 35(4), 345–374.
27. Lancet, D., Kafri, R., & Shenhav, B. (2002). Compositional genomes: Pre-RNA information transfer in mutually catalytic assemblies. *Geochimica et Cosmochimica Acta*, 66(15A), A429–A429.
28. Lancet, D., Kedem, O., & Pilpel, Y. (1994). Emergence of order in small autocatalytic sets maintained far from equilibrium—Application of a probabilistic receptor affinity distribution (RAD) model. *Berichte der Bunsen-Gesellschaft—Physical Chemistry Chemical Physics*, 98(9), 1166–1169.
29. Lancet, D., Sadovsky, E., & Seidemann, E. (1993). Probability model for molecular recognition in biological receptor repertoires—Significance to the olfactory system. *Proceedings of the National Academy of Sciences of the United States of America*, 90(8), 3715–3719.
30. Lee, D. H., Severin, K., Yokobayashi, Y., & Ghadiri, M. R. (1997). Emergence of symbiosis in peptide self-replication through a hypercyclic network. *Nature*, 390, 591–594.
31. Lifson, S. (1997). On the crucial stages in the origin of animate matter. *Journal of Molecular Evolution*, 44, 1–8.
32. Lifson, S., & Lifson, H. (1999). A model of prebiotic replication: Survival of the fittest versus extinction of the unfittest. *Journal of Theoretical Biology*, 199(4), 425–433.
33. Limpert, E., Stahel, W. A., & Abbt, M. (2001). Log-normal distributions across the sciences: Keys and clues. *Bioscience*, 51(5), 341–352.
34. Luisi, P. L., Walde, P., & Oberholzer, T. (1999). Lipid vesicles as possible intermediates in the origin of life. *Current Opinion in Colloid & Interface Science*, 4(1), 33–39.
35. McMullin, B. (2000). Remarks on autocatalysis and autopoiesis. *Annals of the New York Academy of Sciences*, 901(1), 163–174.
36. Moran, P. A. P. (1958). Random processes in genetics. *Mathematical Proceedings of the Cambridge Philosophical Society*, 54, 60–71.
37. Muller, U. F. (2006). Re-creating an RNA world. *Cellular and Molecular Life Sciences*, 63(11), 1278–1293.
38. Naveh, B., Sipper, M., Lancet, D., & Shenhav, B. (2004). Lipidia: An artificial chemistry of self-replicating assemblies of lipid-like molecules. In *9th International Conference on the Simulation and Synthesis of Living Systems (ALIFE9)* (pp. 466–471).
39. Norris, V., Hunding, A., Kepes, F., Lancet, D., Minsky, A., Raine, D., Root-Bernstein, R., & Sriram, K. (2007). The first units of life were not simple cells. *Origins of Life and Evolution of Biospheres*, 37(4–5), 429–432.
40. Orgel, L. (2000). Origin of life—A simpler nucleic acid. *Science*, 290, 1306–1307.

41. Orgel, L. E. (1992). Molecular replication. *Nature*, *358*, 203–209.
42. Orgel, L. E. (2004). Prebiotic chemistry and the origin of the RNA world. *Critical Reviews in Biochemistry and Molecular Biology*, *39*(2), 99–123.
43. Pigliucci, M. (2008). Opinion—Is evolvability evolvable? *Nature Reviews Genetics*, *9*(1), 75–82.
44. Plasson, R., Brandenburg, A., Jullien, L., & Bersini, H. (2010). Autocatalyses. In H. Fellermann, M. Dorr, M. Hanczyc, L. Laursen, S. Maurer, D. Merkle, P. Monnard, K. Stoy, & S. Rasmussen (Eds.), *Twelfth International Conference on the Synthesis and Simulation of Living Systems* (pp. 4–11). Cambridge, MA: MIT Press.
45. Rasmussen, S., Bedau, M. A., Chen, L., Deamer, D., Krakauer, D. C., Packard, N. H., & Stadler, P. F. (Eds.). (2009). *Protocells: Bridging nonliving and living matter* (p. 684). Cambridge, MA: MIT Press.
46. Rosenwald, S., Kafri, R., & Lancet, D. (2002). Test of a statistical model for molecular recognition in biological repertoires. *Journal of Theoretical Biology*, *216*(3), 327–336.
47. Schuster, P., & Stadler, F. (2003). Networks in molecular evolution. *Complexity*, *8*(1), 34–42.
48. Segre, D., Ben-Eli, D., Deamer, D. W., & Lancet, D. (2001). The lipid world. *Origins of Life and Evolution of the Biosphere*, *31*(1–2), 119–145.
49. Segre, D., Ben-Eli, D., & Lancet, D. (2000). Compositional genomes: Prebiotic information transfer in mutually catalytic noncovalent assemblies. *Proceedings of the National Academy of Sciences of the United States of America*, *97*(8), 4112–4117.
50. Segre, D., & Lancet, D. (2000). Composing life. *Embo Reports*, *1*(3), 217–222.
51. Segre, D., Lancet, D., Kedem, O., & Pilpel, Y. (1998). Graded autocatalysis replication domain (GARD): Kinetic analysis of self-replication in mutually catalytic sets. *Origins of Life and Evolution of the Biosphere*, *28*(4–6), 501–514.
52. Segre, D., Shenhav, B., Kafri, R., & Lancet, D. (2001). The molecular roots of compositional inheritance. *Journal of Theoretical Biology*, *213*(3), 481–491.
53. Shapiro, R. (2006). Small molecule interactions were central to the origin of life. *Quarterly Review of Biology*, *81*(2), 105–125.
54. Shapiro, R. (2007). A simpler origin for life. *Scientific American*, *296*(4), 46–53.
55. Shenhav, B., Bar-Even, A., Kafri, R., & Lancet, D. (2005). Polymer GARD: Computer simulation of covalent bond formation in reproducing molecular assemblies. *Origins of Life and Evolution of the Biosphere*, *35*(2), 111–133.
56. Shenhav, B., Oz, A., & Lancet, D. (2007). Coevolution of compositional protocells and their environment. *Philosophical Transactions of the Royal Society B—Biological Sciences*, *362*, 1813–1819.
57. Shenhav, B., Solomon, A., Lancet, D., & Kafri, R. (2005). Early systems biology and prebiotic networks. *Transactions on Computational Systems Biology*, *1*, 14–27.
58. Silvestre, D. A. M. M., & Fontanari, J. F. (2008). The information capacity of hypercycles. *Journal of Theoretical Biology*, *254*(4), 804–806.
59. Sole, R. V., Rasmussen, S., & Bedau, M. (2007). Introduction. Artificial protocells. *Philosophical Transactions of the Royal Society B—Biological Sciences*, *362*, 1725–1725.
60. Stadler, P. F. (1991). Dynamics of autocatalytic reaction networks. 4. Inhomogeneous replicator networks. *Biosystems*, *26*(1), 1–19.
61. Steinley, D. (2006). K-means clustering: A half-century synthesis. *British Journal of Mathematical & Statistical Psychology*, *59*, 1–34.
62. Szathmáry, E. (1995). A classification of replicators and lambda-calculus models of biological organization. *Proceedings of the Royal Society B—Biological Sciences*, *260*(1359), 279–286.
63. Szathmáry, E., Santos, M., & Fernando, C. (2005). Evolutionary potential and requirements for minimal protocells. *Topics in Current Chemistry*, *259*, 167–211.
64. Szathmáry, E., & Smith, J. M. (1997). From replicators to reproducers: The first major transitions leading to life. *Journal of Theoretical Biology*, *187*(4), 555–571.
65. Thomas, J. A., & Rana, F. R. (2007). The influence of environmental conditions, lipid composition, and phase behavior on the origin of cell membranes. *Origins of Life and Evolution of Biospheres*, *37*(3), 267–285.

66. Ullrich, A., Rohrschneider, M., Scheuermann, G., Stadler, P. F., & Flamm, C. (2011). In silico evolution of early metabolism. *Artificial Life*, 17(2), 87–108.
67. Varela, F. G., Maturana, H. R., & Uribe, R. (1974). Autopoiesis: The organization of living systems, its characterization and a model. *Biosystems*, 5(4), 187–196.
68. Vasas, V., Szathmáry, E., & Santos, M. (2010). Lack of evolvability in self-sustaining autocatalytic networks constrains metabolism—First scenarios for the origin of life. *Proceedings of the National Academy of Sciences of the United States of America*, 107(4), 1470–1475.
69. Weber, A. L. (2000). Sugars as the optimal biosynthetic carbon substrate of aqueous life throughout the universe. *Origins of Life and Evolution of the Biosphere*, 30(1), 33–43.
70. Wu, M., & Higgs, P. G. (2008). Compositional inheritance: Comparison of self-assembly and catalysis. *Origins of Life and Evolution of Biospheres*, 38(5), 399–418.

## Appendix

### A.1 Distribution and Sampling of the GARD Matrix $\beta$

While not much is known about the values of the rate enhancement between prebiotic molecules, there is a need to consider such values by a physically reasonable method.  $\beta_{ij}$  values are randomly generated based on a lognormal distribution

$$P(\beta_{ij}) = \frac{1}{\beta_{ij}\sigma\sqrt{2\pi}} \exp\left(-\frac{(\ln \beta_{ij} - \mu)^2}{2\sigma^2}\right) \quad (12)$$

where  $\mu$  and  $\sigma$  are the mean and standard deviation, respectively, which can be considered as a “natural” distribution [33], in accordance with the receptor affinity distribution formalism [28, 29, 46], and it was also shown that a lognormal  $\beta$  increases the reproduction fidelity over the normal  $\beta$  in GARD [52]. Each randomization of the  $\beta$  network may be thought of as representing the relative rates of the  $N_G$  molecules as they might ensue from different possible GARD environments.

Self-catalysis in GARD is represented by



Often self-catalysis is written as [4]



The seeming dichotomy between the notations  $\beta_{ii}$  and  $\beta_{XY}$  is clarified on noting that in the GARD, molecules have two states, *in* and *out*, which behave as distinct chemical species. While it is possible that more complex pathways would also be autocatalytic [44], this work refers to self-catalysis as the simplest closed subnetwork of the  $\beta$  network, containing one element (Figure 1).

### A.2 Fitting the Similarity Autocorrelation Function

The fitting procedure is as follows: (1) Calculate  $H_0$  as the mean of  $c(\Delta t)$  in the interval  $[GEN/4, GEN/2]$ . (2) Guess  $\tau^\ddagger$  as the first instance  $c(\Delta t)$  drops below  $H_0$ . (3) Smooth the  $c(\Delta t)$  tail by forcing:  $c(\Delta t > \tau^\ddagger) = H_0$ . (4) Fit an exponential (Equation 7) to the smoothed  $c(\Delta t)$ , using nonlinear least squares with a tolerance of  $10^{-5}$ .

Examples are given in Figure 12 in Appendix A.4.

### A.3 $p$ -Values

See Table 2.

**Table 2.** Student’s  $t$ -test statistical analysis for the selection excess of  $\beta$  networks exhibiting  $p_{mc} > 100$  (Equations 4 and 10). Test was run using MATLAB function `ttest`, against the null hypothesis that the data are a random sample from a normal distribution with mean 1.0, per specific ranges of lognormal random seeds.

Random-seed range	$p_{mc} > 100^*$	Selection excess <sup>†</sup>	$p$ -Value
50–300	3	$0.973 \pm 0.0395$	$3.57 \times 10^{-1}$
300–800	5	$1.311 \pm 0.389$	$1.49 \times 10^{-1}$
1,000–3,500	40	$1.100 \pm 0.325$	$5.95 \times 10^{-2}$
5,000–10,000	70	$1.119 \pm 0.248$	$1.45 \times 10^{-4}$
1–10,000	143	$1.105 \pm 0.272$	$8.03 \times 10^{-6}$

\*The number of networks exhibiting high  $p_{mc}$  value.

†Mean and standard deviation of the selection excess of these networks (under regular GARD simulations).

### A.4 Examples

See Figures 10–14.

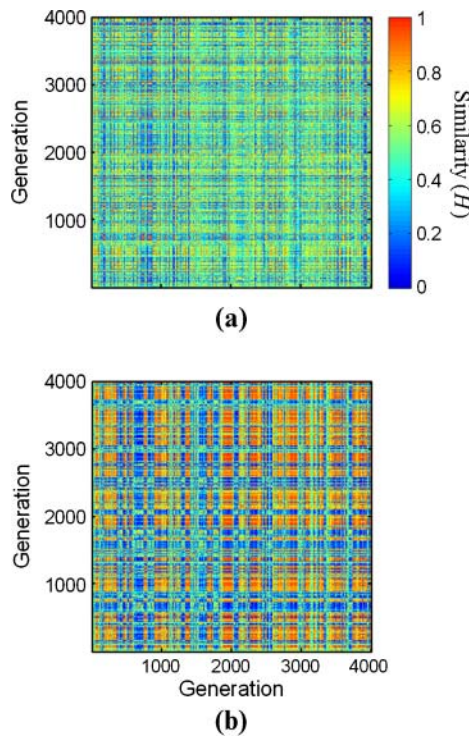


**Figure 10.** Example of carpets from two regular-GARD simulations with lognormal seeds 42 and 41 (a and b, respectively) and the rest of the parameters as in Table 2. Compotype counts are 4 and 2, respectively.  $\beta$  matrices are presented in Figure 11, and functions  $c(\Delta t)$  in Figure 12.

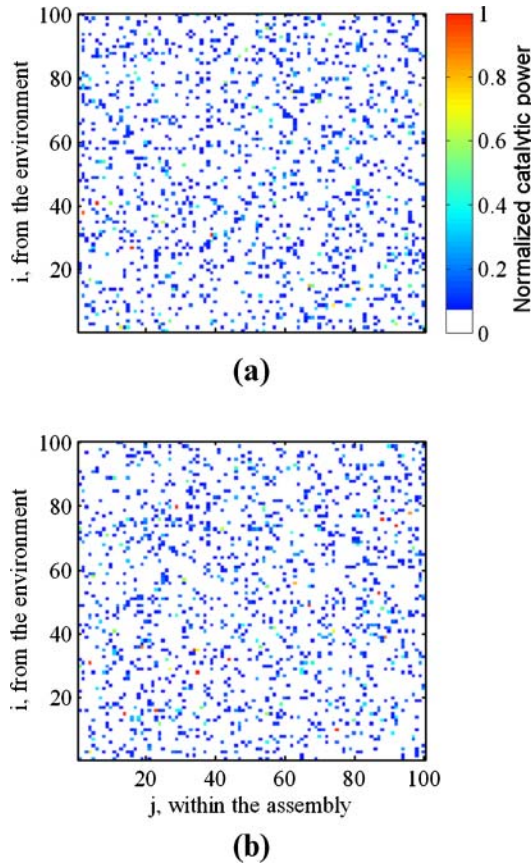


Figure 11.  $\beta$  matrices for the two simulations in Figure 10.  $p_{mc}$  values are 1.98 and 0.81, respectively. To better express the richness of the  $\beta$  matrix, catalytic values are scaled according to  $\beta_{ij} = 2^{\log_{10} \beta_{ij}^0 - 4}$  (values of  $\beta_{ij}^0$  are generated according to Equation 12).

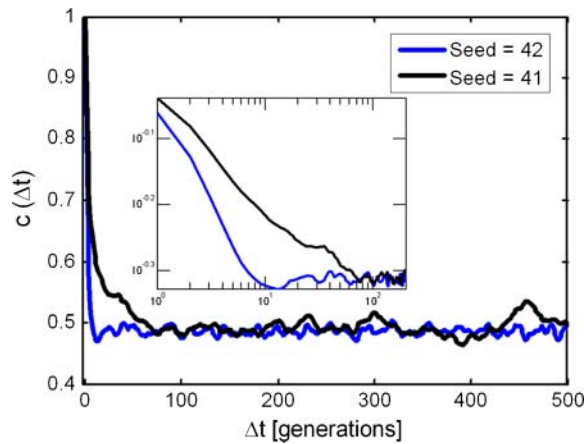


Figure 12. Functions  $c(\Delta t)$  for the two simulations in Figure 10. Insert shows initial decay on a log-log scale. Fitted parameters for Equation 7 are  $\tau = 2.57$ ,  $H_0 = 0.49$  (seed = 41), and  $\tau = 6.32$ ,  $H_0 = 0.50$  (seed = 42).

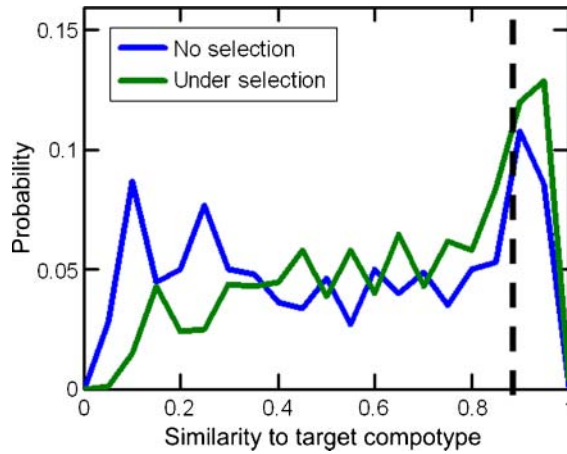


Figure 13. Example histograms of similarity between the target compotype from a regular GARD simulation, for a population of 1,000 assemblies, with and without selection. A cutoff of  $H \geq 0.9$  (dashed line) is imposed to identify the frequency of the compotype in the GARD population. Simulation details are lognormal seed = 3, GEN = 5,000, and the rest as in Table 2.

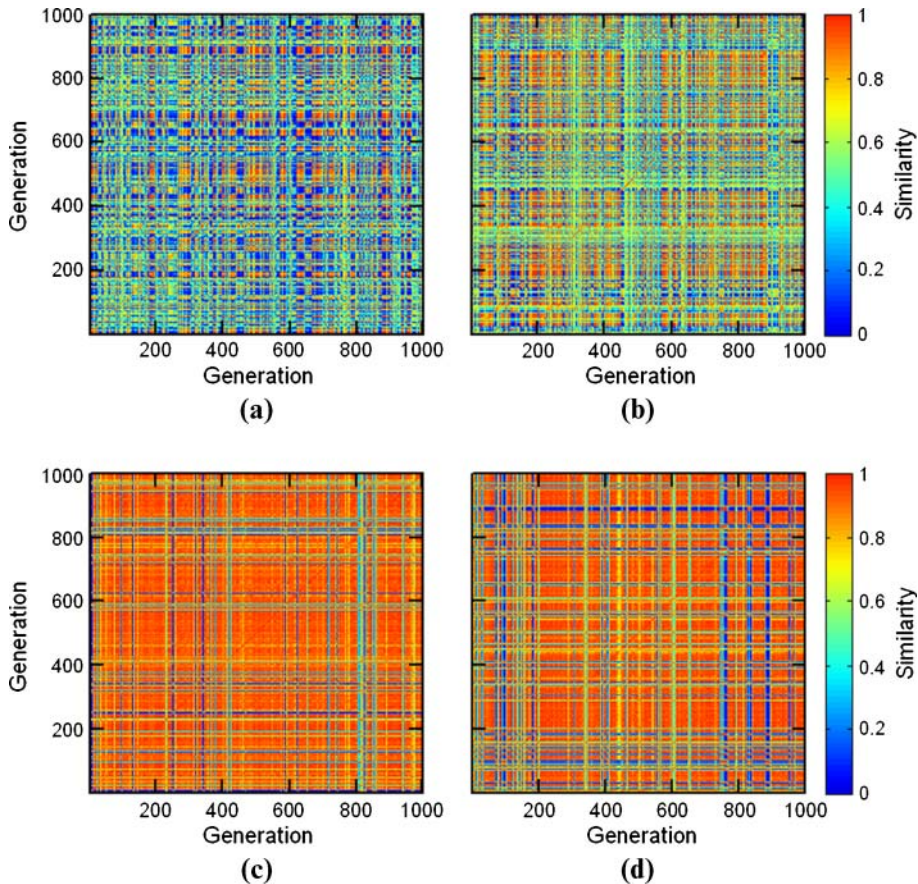


Figure 14. Regular-GARD similarity carpets before and after selection. (a) Similarity carpet of the GARD instance generated with lognormal seed 114. The frequency of the target compotype is  $f_T = 0.27$ . (b) The same carpet as (a), after applying selection pressure, whereby the new frequency of the target is  $f_T = 0.34$ . (c) Similarity carpet of the GARD instance generated with lognormal seed 168. Here  $f_T = 0.82$ . (d) The results after applying selection pressure. Here  $f_T = 0.74$ . Simulation parameters are in Table 1.

Downloaded from [http://direct.mit.edu/artlife/article-pdf/18/3/243/1663284/artl\\_a\\_00064.pdf](http://direct.mit.edu/artlife/article-pdf/18/3/243/1663284/artl_a_00064.pdf) by guest on 09 May 2021

### A.5 Selection Excess and the Number of Comptypes

See Figures 15–16.

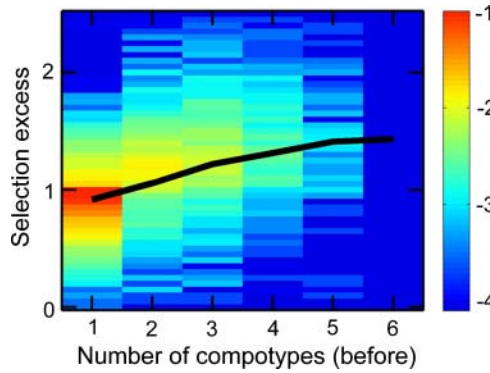


Figure 15. The dependence of selection excess on the number of comptypes (before selection). Black solid line plots the average selection excess per comptype count. Figure details are as in Figure 2a.

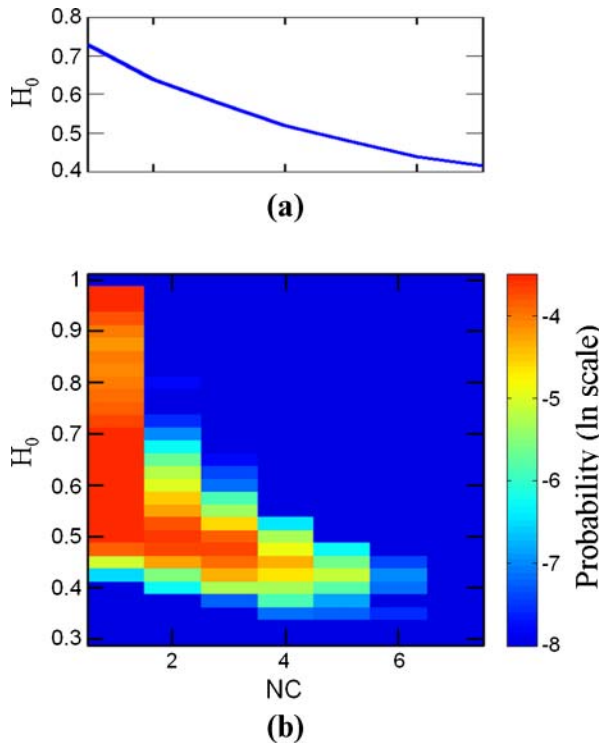


Figure 16. The weak dependence of  $H_0$  on the number of comptypes ( $NC$ ). (a) Average  $H_0$  versus  $NC$  after 5-point moving-average smoothing. Fitting the smoothed data to a linear curve gives a slope of  $-0.0485$  with  $r^2 = 0.89$ . (b) Density plot of the probability to have a simulation with a pair of  $H_0$  and  $NC$  values. In the electronic version, the color represents the normalized probability to find a network with such a pair (in scale; red means that about 300 simulations fall in this bin). Simulation parameters are as in Figure 15.

### A.6 Assembly Size

See Figures 17 and Table 3.

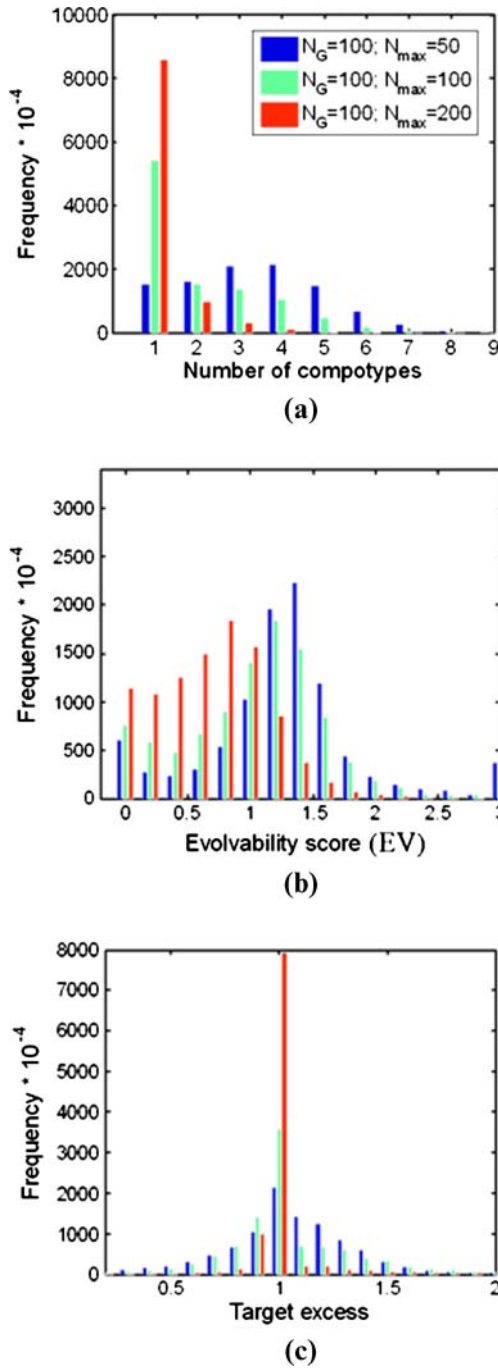


Figure 17. Histograms of the three evolution-related parameters, per  $N_{max}$  values. (a) Number of comptypes (NC). In the electronic version, blue bars are with  $N_{max} = N_G/2$ , green bars are with  $N_{max} = N_G$ , and red bars are with  $N_{max} = 2N_G$ . The rest of parameters are as in Figure 15. (b) Evolvability score (EV). (c) Selection excess (SE).

**Table 3.** Mean values collected from Figure 17. Number in parenthesis refers to the percentage of simulations that show positive or negative selection.

Number	Mean value		
	$N_{\max} = 2N_G$	$N_{\max} = N_G$	$N_{\max} = N_G/2$
NC	1.20	2.03	3.38
EV	0.72	1.11	1.35
SE	1.01	1.05	1.04
SE > 1.05	1.36 (8%)	1.38 (33%)	1.28 (48%)
SE < 0.95	0.85 (13%)	0.77 (31%)	0.71 (30%)